Journal of Power Sources 253 (2014) 392–396

Contents lists available at ScienceDirect

Journal of Power Sources

journal homepage: www.elsevier.com/locate/jpowsour

Short communication

The effect of ethanol concentration on the direct ethanol fuel cell performance and products distribution: A study using a single fuel cell/attenuated total reflectance – Fourier transform infrared spectroscopy

M.H.M.T. Assumpção, J. Nandenha, G.S. Buzzo, J.C.M. Silva, E.V. Spinacé, A.O. Neto, R.F.B. De Souza*

Instituto de Pesquisas Energéticas e Nucleares, IPEN-CNEN/SP, Av. Prof. Lineu Prestes, 2242 Cidade Universitária, CEP 05508-900 São Paulo, SP, Brazil

HIGHLIGHTS

- The power density increases with the ethanol concentration until 1 mol L^{-1}.
- The maximum power density is a result of acetic acid production using Pt_3Sn_1/C.
- The 2 mol L^{-1} ethanol solution showed small power density due to the crossover.

ARTICLE INFO

Article history:
Received 16 October 2013
Received in revised form
3 December 2013
Accepted 18 December 2013
Available online 27 December 2013

Keywords:
DEFC
Ethanol concentration
PtSn/C
DEFC/ATR-FTIR

ABSTRACT

The effect of ethanol concentration on the direct ethanol fuel cell (DEFC) performance and products distribution were studied in situ using a single fuel cell/ATR-FTIR setup. The experiments were performed at 80 °C using commercial Pt_3Sn/C as anodic catalyst and the concentrations of ethanol solution were varied from 0.1 to 2.0 mol L^{-1}. An increase in power density was observed with the increase of ethanol concentration to 1.0 mol L^{-1}, while the band intensities analysis in the FTIR spectra revealed an increase of acetic acid/acetaldehyde ratio with the increase of ethanol concentration. Also, from FTIR spectra results, it could be concluded that the acetic acid production follow parallel mechanisms; that is, it does not require the presence of acetaldehyde as an intermediate.

1. Introduction

Direct ethanol fuel cells (DEFCs) research is becoming more popular because ethanol is a green fuel and can be readily and easily produced in great quantity by fermentation of sugar-containing raw materials as sugar cane. Furthermore, this alcohol has low pollutant emitting feature, it has easy fuel delivery and storage, it is directly fed without reforming and it has favorable power capability, compared to the other fuels [1,2]. However, the major difficult in the commercialization of the DEFCs is the lack of catalysts that could promote the complete electro-oxidation of ethanol, forming CO_2 [1,3].

To study the effects of each electrocatalyst in the ethanol oxidation reaction (EOR) pathways, the in situ Fourier transformed infrared (FTIR) spectroscopy is used. The measurements of in situ FTIR can be carried out using different techniques such as reflection–absorption spectroscopy (FTIR-RAS) [4–6], surface enhanced infrared absorption spectroscopy (SEIRAS) [7,8], and a variation of FTIR-RAS using an ATR accessory [9]. Until this point, all techniques presented are only used to study the electrocatalysts, refraining from discussing the participation of the support where this catalyst was deposited.

De Souza et al. [10] used a variation of FTIR-RAS using an ATR accessory (previously mentioned) in order to study different substrates (working electrode) and reported that the catalytic activity toward EOR depends not only on the electrocatalyst but also on various electrodes factors. Then, if these factors change the reaction pathways, it is reasonable to expect that an extrapolation of what is

* Corresponding author. Tel.: +55 11 3133 9284.
E-mail address: souza.rfb@gmail.com (R.F.B. De Souza).

0378-7753/$ – see front matter © 2013 Elsevier B.V. All rights reserved.
http://dx.doi.org/10.1016/j.jpowsour.2013.12.088

seen on a smooth electrode is not entirely valid for what happens in a fuel cell. By this way, recently in the literature was presented a Single Fuel Cell/ATR-FTIR setup [11].

Among the various electrocatalysts tested in the literature, studies have indicated that PtSn/C is the best catalyst for the EOR [12–14], because the Sn is potentially able to provide O-species for the oxidation of intermediates produced during the dissociative adsorption of ethanol on Pt active sites (bi-functional mechanism) [15–17], and in alloyed phase with Pt strengthens the electronic effect [15]. These two points are responsible for improving the activity of PtSn toward EOR [16]. Beyond the catalyst, the conditions of the single fuel cell parameter of operating are very important to the development of its device.

Considering the aspects that affect the fuel cell performance, many authors [18–23] point the concentration as one of the key parameters. In this sense, this study sought to investigate the effect of ethanol concentration on the reaction pathways and how it affects the power density and products distribution in a DEFC.

2. Experimental

Single direct ethanol cell tests were carried out using Pt_3Sn_1/C BASF (20 wt.%) electrocatalyst as anode and Pt/C BASF (20wt.%) as cathode in the gas diffusion electrodes. The electrocatalysts were painted over the gas diffusion layer (GDL – Carbon Paper Teflon treated and Electrochem EC-TP1-060T) in order to obtain an homogeneous dispersion made with Nafion® solution (5 wt.%, Aldrich) and isopropanol (J.T. Baker).

All electrodes were constructed with 1 mg Pt cm^{-2} in the anode and cathode. After preparation, the electrodes were hot pressed on both sides of a Nafion® 117 membrane at 100 °C for 2 min under a pressure of 225 kgf cm^{-2}. Prior to use, the membranes were exposed to 3 wt.% H_2O_2, washed with distilled water and treated with 0.5 mol L^{-1} H_2SO_4.

The performance and ATR-FTIR in-situ spectroscopy of the ethanol fuel cell was investigated using a single Fuel Cell/ATR-FTIR setup [11] with a geometric area of 1 cm^2, adapted in an ATR accessory (MIRacle with a Diamond/ZnSe Crystal Plate Pike®) installed on a Nicolet® 6700 FT-IR spectrometer equipped with a MCT detector cooled with liquid N2. The temperature was set to 80 °C for the fuel cell and for the oxygen humidifier. The fuel in different concentrations (0.1, 0.5, 1, and 2 mol L^{-1} ethanol aqueous solutions) was delivered at 0.8 mL min^{-1} and the oxygen flow was set to 150 mL min^{-1}, operating at 80 °C.

The polarization curves were obtained using an Autolab PGSTAT 302N Potentiostat. Absorbance spectra were collected as the ratio (R:R_0) where R represents a spectrum at a given potential and R_0 is the spectrum collected at an open-circuit voltage (OCV). Negative and positive bands represent the consumption and production of substances, respectively.

3. Results and discussion

In Fig. 1 the polarization and power density curves for a DEFC operating with different concentrations of ethanol solution (0.1, 0.5, 1, and 2 mol L^{-1}) are presented. By this figure it is possible to observe that the open-circuit voltage is very similar for all concentrations. As expected, the increase of ethanol concentration practically does not alter the over potential of the EOR. However, an increase in power density was observed with the increase of ethanol concentration until 1 mol L^{-1}. Similar results were already described by Heysiattalab et al. [23] using a PtRu/C catalyst and Song et al. [19] using PtSn/C catalyst in a single fuel cell, which also observed an increase in the reaction rate in function of the alcohol concentration and considered that the increase of ethanol

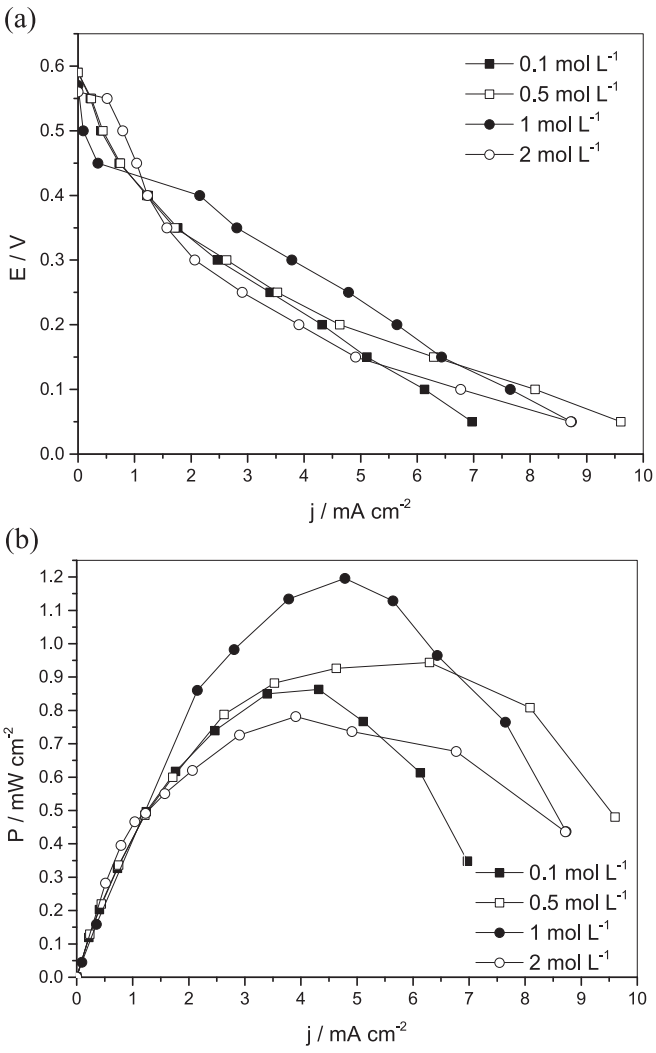

Fig. 1. Polarization curves (a) and power density curves (b) in 1 cm^2 DEFC using 20 wt.% Pt_3Sn_1/C electrocatalyst in the anode and Pt/C at the cathode (1 mg_{Pt} cm^{-2}). Nafion® 117 was used as the membrane.

concentration could facilitate its diffusion to the active sites on the catalyst layer.

Nevertheless, increasing the concentration to 2 mol L^{-1} it makes the power density decrease. This result was also observed by Heysiattalab et al. [23] and Song et al. [19] and could be related to the increase in ethanol crossover to the cathode side what reduces the power density.

The ATR-FTIR spectra (Fig. 2) were acquired during the experiments of polarization curves (Fig. 1) on the anode side of the single fuel cell operating with different ethanol solution concentrations and correspond to solved species in the fuel solution. By these results, it is possible to observe a decrease in the ethanol bands (1053, 1075, and 1090 cm^{-1}) [24] with the decrease in the potential, and consequently, an increase in the bands resulting from acetaldehyde (1339 cm^{-1}) [25] and acetic acid (1436 cm^{-1}) formation [24]. CO_2 signal (2343 cm^{-1}) [21] was not detected in these spectra.

During the fuel cell experiments, as the concentration increases there was an increase in the ethanol consumption (negative bands) and consequently there was also an increase in the power density that is a result linked with the better diffusion of the fuel in the catalytic layer [18,23]. In order to evaluate the concentration effect in the products with the application of different potentials, all bands were deconvoluted to lorentzian line forms [11].

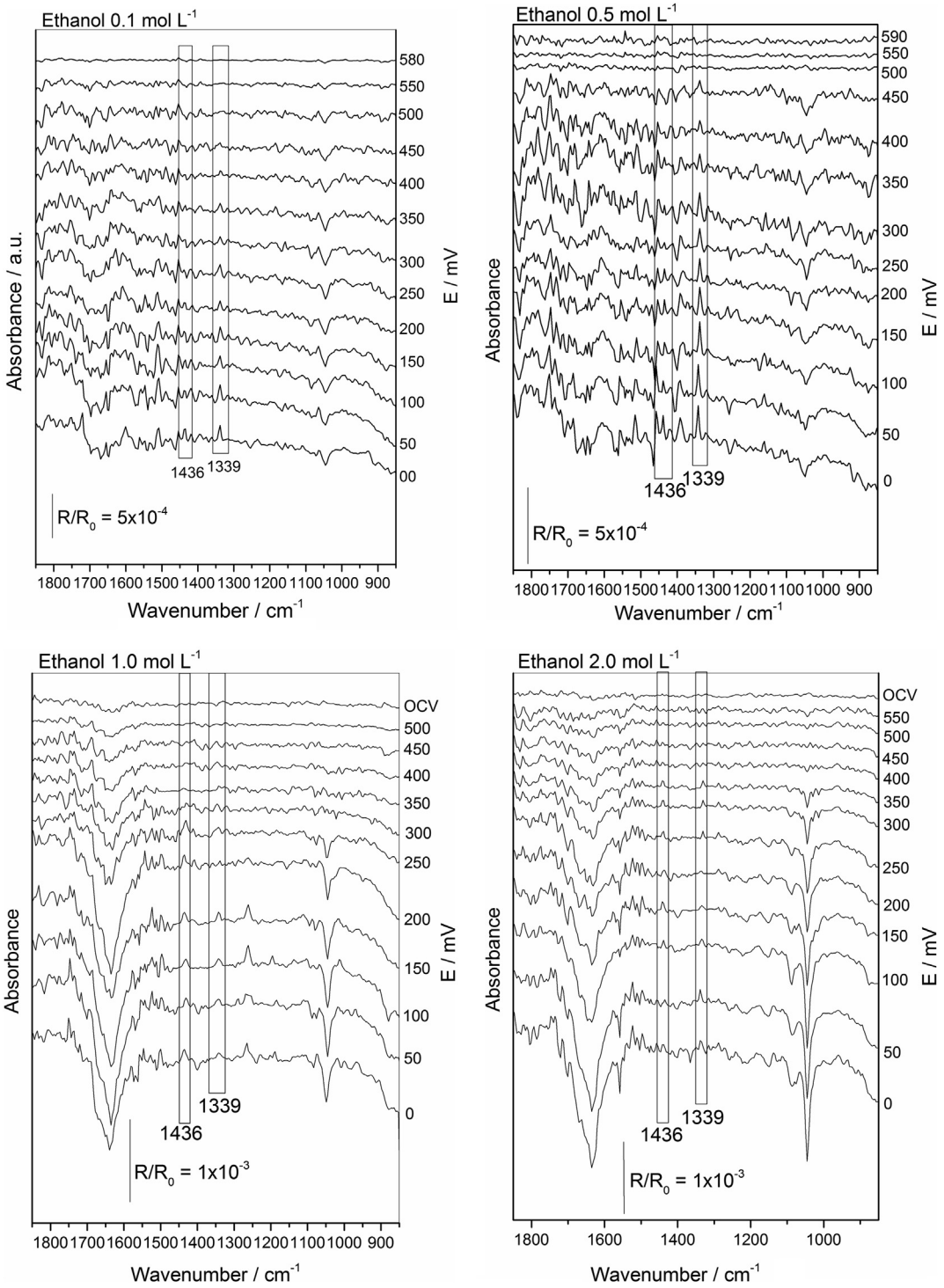

Fig. 2. In situ ATR-FTIR spectra taken at OCV to 0 V in 1.0 cm^{-2} DEFC using 20 wt.% Pt_3Sn_1/C Basf electrocatalyst in anode and Pt/C Basf in cathode (1.0 mg_{Pt} cm^{-2}). Nafion® 117 was used as the membrane. Ethanol solution delivered at 0.8 mL s^{-1}. The backgrounds were collected at OCV.

From the deconvolution results it was possible to observe that the onset potential for acetaldehyde and acetic acid production were simultaneous and close to the OCV for each concentration. This may indicate that the acetic acid formation can be followed by parallel mechanisms; in other words, the presence of acetaldehyde as intermediate is not required [11,21,26].

Considering the recent literature, it has been reported that the EOR can occur by different pathways (Fig 4) and the reaction is complete when CO_2 is the final product, yielding twelve electrons per ethanol molecule. However, the formation of partially oxidized products (such as acetaldehyde and acetic acid) is favored in a wide range of catalysts [27] due to the difficulty of breaking the C–C bond. In the presented work, the formation of partially oxidized species was evidenced by no detection of CO_2 in any of the experimental conditions used.

About the acetaldehyde behavior observed in Fig. 3, for the ethanol solutions at 0.5 and 1 mol L^{-1} it is seen that for the cell potential close to 100 mV, the aldehyde bands start decreasing

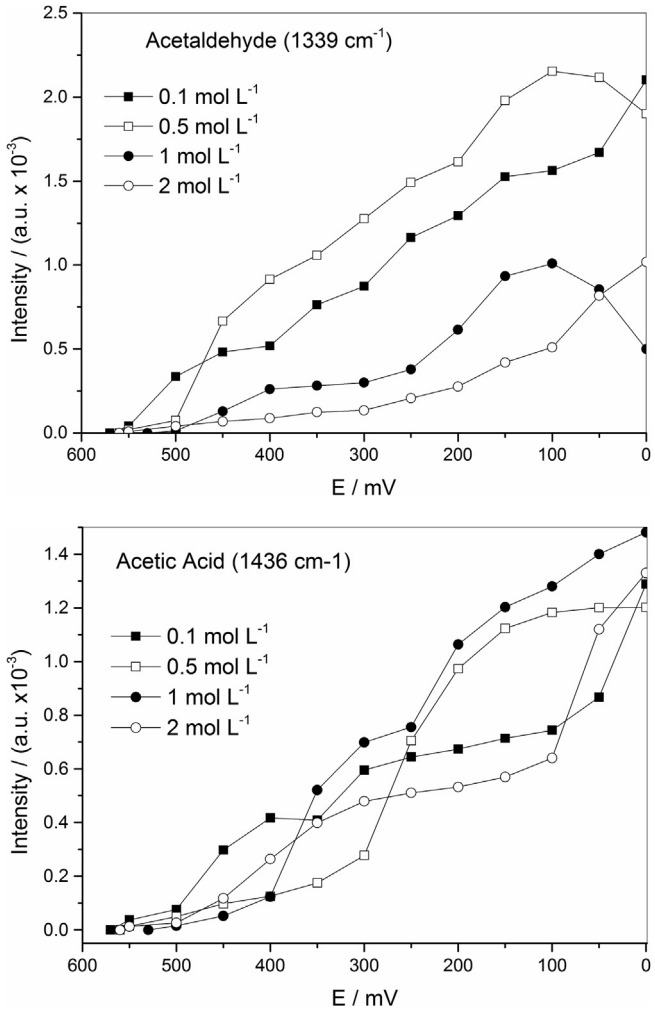

Fig. 3. Integrated band intensity for acetic acid and acetaldehyde as function of potential for the different concentrations using Pt_3Sn_1 electrocatalysts (Data extracted from Fig. 2.).

which can be explained in two ways: i) the acetaldehyde formed could be oxidized to acetic acid ii) using these conditions the catalyst favors the acetic acid production instead of acetaldehyde.

Aiming to obtain a comparative relation between the power density and the products distribution, the integrated band intensity ratio for the acetic acid and acetaldehyde was plotted at 200 mV in function of ethanol concentration. This potential was chosen because it corresponds to the potential of maximum power density for all ethanol concentrations studied. From this figure, it is possible to observe that with the increase of the ethanol concentration there is also an increase in the maximum power density. However, in

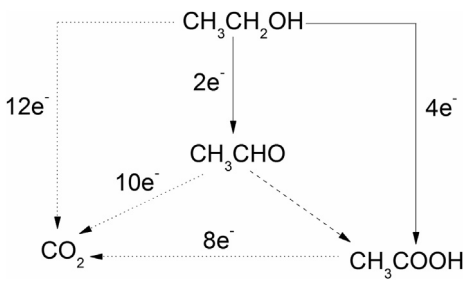

Fig. 4. Mechanism for ethanol oxidation reaction.

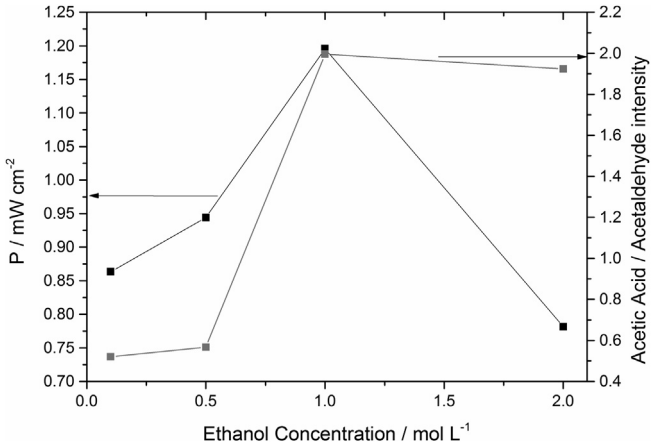

Fig. 5. Acetic acid/acetaldehyde band intensity ratios at 200 mV (data extracted from Fig. 3), and maximum power density (data extracted of Fig. 1b) as function of the concentration.

Fig. 5 it was possible to observe an increase of acetic acid/acetaldehyde intensity bands ratio in function of ethanol concentration. This fact may indicate that the increase of ethanol concentration favored the production route of acetic acid in detriment of the acetaldehyde production what could be associated with the increase in power density since the production of acetic acid yields 4 electrons while the acetaldehyde production yields just 2 electrons per ethanol molecule.

When analyzing the acetic acid/acetaldehyde ratio to 1 and 2 mol L^{-1} of ethanol aqueous solutions, it is possible to observe that there was little variation, but with great impact on maximum power density obtained from the fuel cell, what could be attributed to the increase in the crossover with the increase of the fuel concentration [19,23] and what has no direct relationship with the changes in the EOR pathways in the anode.

4. Conclusion

The increase in power densities with the increase of ethanol solution concentration could be attributed to kinetic and diffusion factors. However, from certain values of ethanol concentration a decrease in the cell performance was observed and could be attributed to the increase in ethanol crossover. Moreover, the FTIR spectra showed that the increase in the power densities can be associated to the increase of acetic acid production and its production follows parallel mechanisms; what means that it does not require the presence of acetaldehyde as an intermediate.

Acknowledgments

The authors thank FAPESP (2011/18246-0, 2012/03516-5, 2012/22731-4, 2013/01577-0) and CNPq (150639/2013-9) for financial support.

References

[1] A. Dutta, S.S. Mahapatra, J. Datta, Int. J. Hydrogen Energy 36 (2011) 14898–14906.
[2] W.J. Zhou, B. Zhou, W.Z. Li, Z.H. Zhou, S.Q. Song, G.Q. Sun, Q. Xin, S. Douvartzides, M. Goula, P. Tsiakaras, J. Power Sources 126 (2004) 16–22.
[3] Y.H. Chu, Y.G. Shul, Int. J. Hydrogen Energy 35 (2010) 11261–11270.
[4] T. Iwasita, Electrochim. Acta 47 (2002) 3663–3674.
[5] S.-G. Sun, Y. Lin, Electrochim. Acta 44 (1998) 1153–1162.
[6] F. Vigier, C. Coutanceau, F. Hahn, E.M. Belgsir, C. Lamy, J. Electroanal. Chem. 563 (2004) 81–89.
[7] Y.X. Chen, S. Ye, M. Heinen, Z. Jusys, M. Osawa, R.J. Behm, J. Phys. Chem. B 110 (2006) 9534–9544.

[8] T. Sato, K. Kunimatsu, H. Uchida, M. Watanabe, Electrochim. Acta 53 (2007) 1265–1278.
[9] J.C.M. Silva, L.S. Parreira, R.F.B. De Souza, M.L. Calegaro, E.V. Spinacé, A.O. Neto, M.C. Santos, Appl. Catal. B 110 (2011) 141–147.
[10] R.F.B. De Souza, J.C.M. Silva, F.C. Simões, M.L. Calegaro, A.O. Neto, M.C. Santos, Int. J. Electrochem. Sci. 7 (2012) 5356–5366.
[11] A.O. Neto, J. Nandenha, M.H.M.T. Assumpção, M. Linardi, E.V. Spinacé, R.F.B. de Souza, Int. J. Hydrogen Energy 38 (2013) 10585–10591.
[12] E. Antolini, F. Colmati, E.R. Gonzalez, J. Power Sources 193 (2009) 555–561.
[13] E. Antolini, J. Power Sources 170 (2007) 1–12.
[14] F. Colmati, E. Antolini, E.R. Gonzalez, Appl. Catal. B 73 (2007) 106–115.
[15] M. Zhu, G. Sun, Q. Xin, Electrochim. Acta 54 (2009) 1511–1518.
[16] M. Zhu, G. Sun, H. Li, L. Cao, Q. Xin, Chin. J. Catal. 29 (2008) 765–770.
[17] R.F.B. De Souza, L.S. Parreira, D.C. Rascio, J.C.M. Silva, E. Teixeira-Neto, M.L. Calegaro, E.V. Spinace, A.O. Neto, M.C. Santos, J. Power Sources 195 (2010) 1589–1593.
[18] V. Alzate, K. Fatih, H. Wang, J. Power Sources 196 (2011) 10625–10631.
[19] S. Song, W. Zhou, J. Tian, R. Cai, G. Sun, Q. Xin, S. Kontou, P. Tsiakaras, J. Power Sources 145 (2005) 266–271.
[20] G. Li, P.G. Pickup, J. Power Sources 161 (2006) 256–263.
[21] M.J. Giz, G.A. Camara, J. Electroanal. Chem. 625 (2009) 117–122.
[22] J.C.M. Silva, R.F.B. De Souza, M.A. Romano, M. D'Villa-Silva, M.L. Calegaro, P. Hammer, A.O. Neto, M.C. Santos, J. Braz. Chem. Soc. 23 (2012) 1146–1153.
[23] S. Heysiattalab, M. Shakeri, M. Safari, M.M. Keikha, J. Industr. Eng. Chem. 17 (2011) 727–729.
[24] National Institute of Standards and Technology, NIST, in: (http://webbook.nist.gov/cgi/cbook.cgi?Name=acetic+acid&Units=SI).
[25] B. Hauchecorne, D. Terrens, S. Verbruggen, J.A. Martens, H. Van Langenhove, K. Demeestere, S. Lenaerts, Appl. Catal. B 106 (2011) 630–638.
[26] R.M. Piasentin, R.F.B. de Souza, J.C.M. Silva, E.V. Spinacé, M.C. Santos, A.O. Neto, Int. J. Electrochem. Sci. 8 (2013) 435–445.
[27] M.C. Figueiredo, A. Santasalo-Aarnio, F.J. Vidal-Iglesias, J. Solla-Gullón, J.M. Feliu, K. Kontturi, T. Kallio, Appl. Catal. B 140–141 (2013) 378–385.